Directional Wave Spectra from Video Images Data and SWAN Model

Muhammad Zikra[a]*, Noriaki Hashimoto[b], Masaru Yamashiro[b], Kojiro Suzuki[c]

[a]Department of Ocean Engineering, Institut Teknologi Sepuluh Nopember (ITS), Surabaya, Indonesia
[b]Department of Maritime Engineering, Kyushu University, Japan
[c]Port and Airport Research Institute (PARI), Japan

*Corresponding author: mzikro@oe.its.ac.id

Graphical abstract
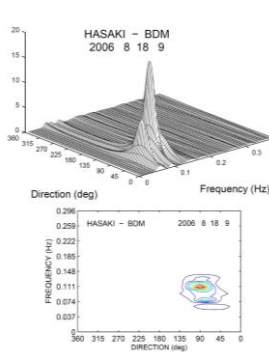
Abstract

In this paper, analysis of directional wave spectra in shallow water area estimated by video images data has been compared with numerical model of SWAN. Estimation of directional wave spectra from video images is based on the Bayesian Directional Method using a group of pixels brightness on the image. For this study, the pixels can be considered equivalent to fixed instruments as wave probe sensor after rectification process. The results show that there is a good agreement between directional wave spectra estimated by video images data and the SWAN model. Both methods estimate similar shape of directional wave spectra in the shallow water. In addition, the energy distribution of directional wave spectra in shallow water is concentrated significantly in frequency and direction.

Keywords: Directional wave spectra; SWAN; video images; pixels

■1.0 INTRODUCTION

Analysis wave conditions in shallow water are a major concern for variety of nearshore processes such as erosion or sediment transport study, and they play important factors in planning and designing of many coastal projects. Numerical modeling is one of the methods which can be carried out to analyze wave conditions in the shallow water. The models of WAM (Wave Model) [1] or SWAN (Simulating Waves Nearshore) [2] are examples of the third generation wave model, which can be used to compute the spectra of random short-crested waves. Specifically, the SWAN wave modeling was developed for coastal and inland water zones.

Shallow water areas are known as a region with high-energy environment, and then conducting research in this area becomes one of the challenges. Recently, there has been considerable interest in applying digital video system for the study of wave parameters in nearshore area. The advantage of video image technique is that the collection of data can be made rapidly and remotely in real time under dynamic conditions of coastal zones. The capability of the video image techniques have been successfully used and developed into a very useful tool for monitoring coastal changes in the nearshore environmental area [3]. Further examples of the applications of video camera system are the study of sand bar morphology [4], foreshore beach slope [5], wave run up [6], wave phase to estimate bathymetry [7][12], directional wave spectra [8] or the study of coastal management [9] and etc.

After we have successfully derived directional wave spectra using the group of pixel brightness of video image data [10], it is important to compare the results of directional spectra using whatever data are available or even with different formulation such as using numerical wave models. Due to the lack of wave measurement data in the shallow water wave, in this work, numerical model of SWAN has been selected to verify the results on directional wave spectra from video images in the shallow water.

■2.0 STUDY AREA

This research study is located on 120 km east of Tokyo facing the North Pacific Ocean as shown in Figure 1 below. During 2006, the yearly average significant wave height ($H_{1/3}$) is about 1.06 m with corresponding wave period ($T_{1/3}$) of 8.4 seconds. In normal condition, waves approach the coast most often from the East and

South East directions. The average of the tidal range is about 1.60 m.
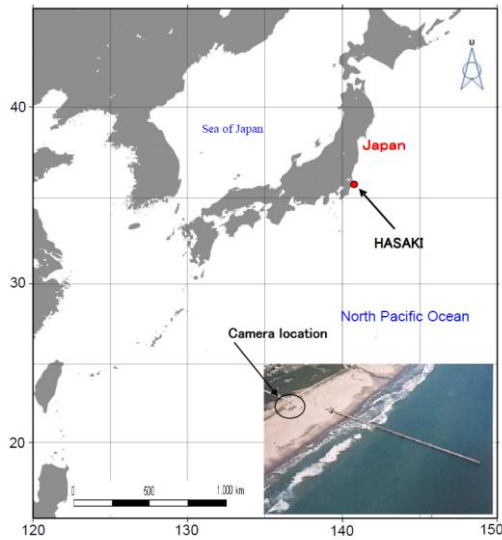
Figure 1 Hasaki site location

■3.0 DATA

Bathymetry in Hasaki beach was measured periodically once or twice a year near HORS pier within area about 600 m alongshore direction and 700 m long in the cross-shore direction. Bathymetry data along alongshore distance are made with interval 50 meters. On each cross-shore transect, measurement are made at a spacing of 10 meters. Map of bathymetry survey conducted on August 2006 is shown in Figure 2. The HORS pier is located at x = 0 m where in-situ pressure wave gauges installed. The HORS pier itself, it is about 427 m long with 3.3 m width of deck.

The actual surface fluctuations in the Hasaki site were recorded using several ultrasonic wave gauges. The ultrasonic wave gauges were installed on the pier with position x = 378 m, x = 230 m, and x = 145 m from the shoreline as shown in Figure 2 above. Water surface fluctuations were recorded as 60 minutes segment, each of which contains approximately 7200 data points, at a sampling rate of 2 Hz.

Meanwhile, image data were collected by using single camera installed in HORS pier at Hasaki beach, Japan in 2006. The digital video camera with the resolution of 640 x 420 pixels was used to acquire snapshot images. This video camera was mounted 10 m high above the ground level. The video images data was recorded for 15 minutes duration at every one hour interval with frequency sampling interval of 1 Hz. Figure 3 shows the example of snapshot images recorded by video camera system around pier area at Hasaki site
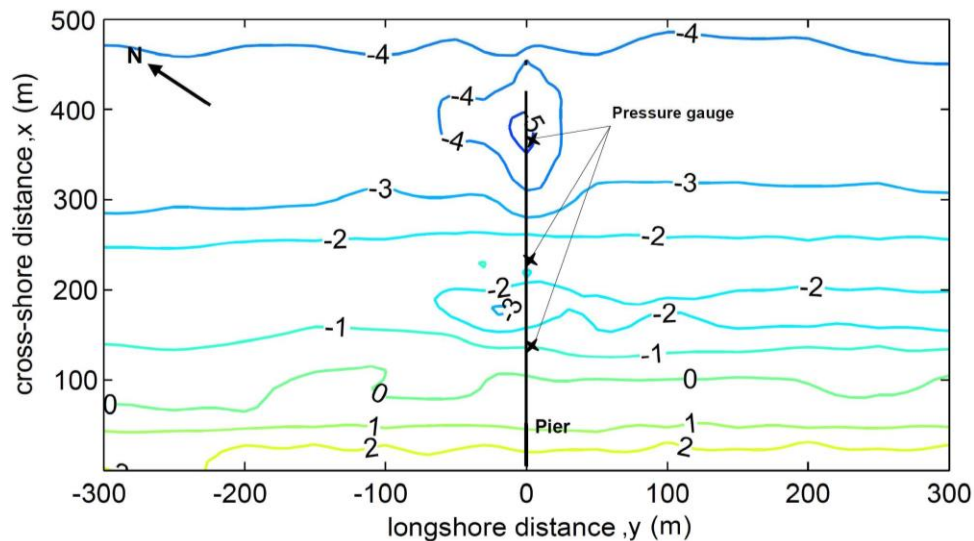
Figure 2 Bathymetry contours from survey measurement conducted on August, 2006 at Hasaki pier. Pressure gauges mounted on pier at x = 145 m, x = 230 m, and x = 378 m from shoreline, respectively
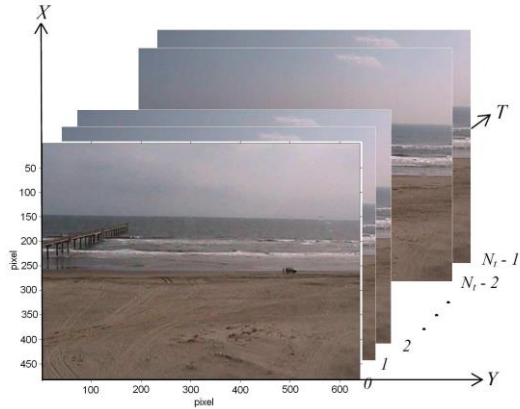
Figure 3 Snapshot image time series

■4.0 SWAN

The model of SWAN is a third generation wave model developed at the Technical University of Delft in the Netherlands [2]. The SWAN model is open source program and is widely used by scientists and engineers for nearshore wave modeling. The model is based on the following spectral action balance equation read as follows:

$$\frac{\partial}{\partial t}N + \frac{\partial}{\partial x}c_x N + \frac{\partial}{\partial y}c_y N + \frac{\partial}{\partial \sigma}c_\sigma N + \frac{\partial}{\partial \theta}c_\theta N = \frac{S_{tot}}{\sigma} \tag{1}$$

With

$$S_{tot} = S_{in} + S_{nl} + S_{wc} + S_{bfr} + S_{surf} \tag{2}$$

in which $N(\sigma,\theta)$ is the action density spectrum. The terms on the left-hand side of Equation 1 represent, respectively, the change of wave action in time, the propagation of wave action in geographic space (with propagation velocities $c_{g,x}$ and $c_{g,y}$ in x- and y-space), the next term represents depth- and current-induced refraction (with propagation velocity c_θ in θ -space (directional space)) and the shifting of the radian frequency σ due to variations in mean depth and current (with the propagation velocity C_σ in σ – space).

For the right-hand side Equation 1 represents processes that generate, dissipate or redistribute wave energy. In deep water, three source terms are employed. These are the transfer of energy from the wind to the waves (S_{in}), the dissipation of wave energy due to white-capping (S_{wc}), and the nonlinear transfer of wave energy due to quadruplet (four-wave) interaction (S_{nl4}), In shallow water, dissipation due to bottom friction (S_{bfr}), depth-induced breaking (S_{surf}), and nonlinear triad (three-wave) interaction, S_{nl3}, are additionally accounted for. Extensive details on the formulations of SWAN code can be found in e.g., Booij *et al.*, (1999) and Ris *et al.*, (1999).

■5.0 RESULTS AND DISCUSSIONS

In the SWAN model, a rectilinear computation grid is used with a grid size of 5 m x 5 m. In order to minimize the effect of lateral boundaries, the computational domains were extended beyond area of interest. The computational grids extend for 900 m

in the cross-shore direction. In the alongshore direction, the computational domains were extended on each side about 600 m. The generated computational grids contain 21.600 grids. In SWAN model, the coastline absorbs all the incoming waves. The wave input conditions for SWAN are defined along the offshore boundary of the rectangular domain (at cross shore distance, $y = 900$ m) as shown in Figure 4. Boundary conditions for SWAN computations used herein are taken from the implementation result of the WAM model [1]. Uniform winds were assumed over the SWAN domain based on average wind measurements at HORS pier. Tidal measurements were also used to adjust the water depth in the model.

In this present study, three nests were used in the WAM model as shown in Figure 5 to generate boundary conditions for SWAN computations, moving from coarser to finer resolution. Table 1 gives information concerning the different nests used for WAM run.
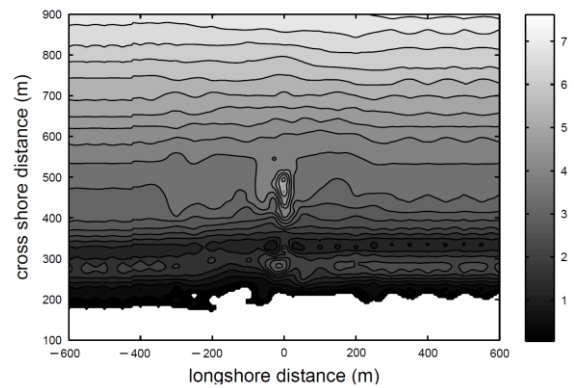
Figure 4 Model domain and bathymetry for SWAN computations

Table 1 Nested grids were used in WAM model

Nest level	Max/min lon. (deg)	Max/min lat. (deg)	Resolution (deg)	Mesh size (m)
Region	122/155	20/47	1-2	1900
Sub 1	137/150	30/43	0.125	237.5
Sub 2	140/145	34/37	0.0625	119
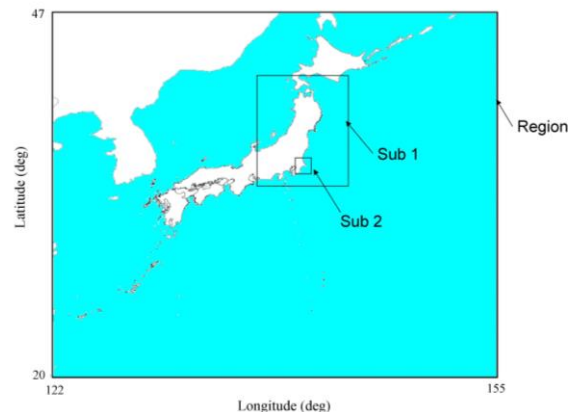
Figure 5 WAM computation areas

For WAM computations above, the bathymetry data for the region was extracted from ETOPO2 from NOAA (National Geographic Data Center, National Oceanic and Atmospheric Administration, USA). Meanwhile, the wind data used to drive the WAM computations nests were obtained from JMA (Japan Meteorological Agency, Japan). The wind field includes both forecast and hindcast, its domain covers the latitudes 20°N – 47°N and longitudes 122°E-155°E. The input of wind time step is 60 minutes.
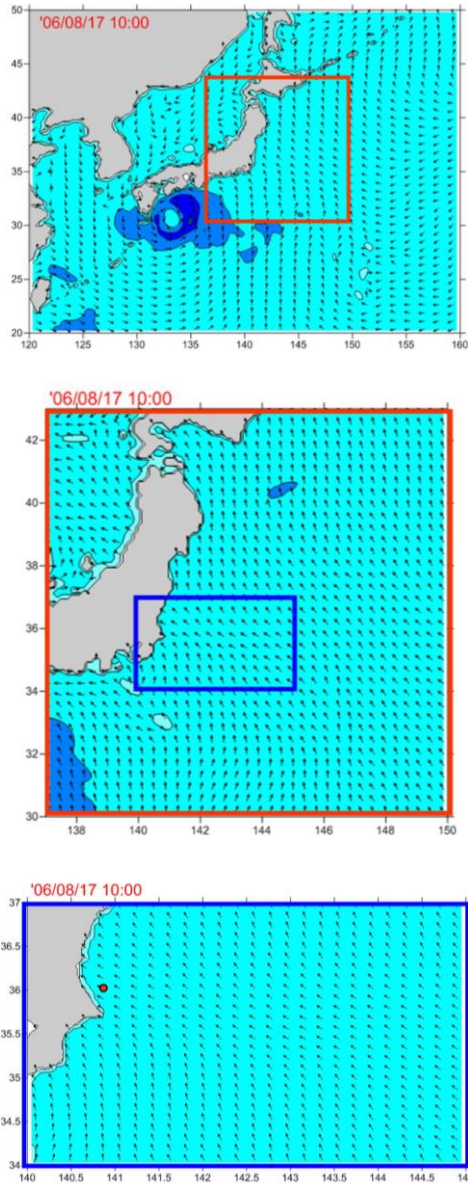
Figure 6 WAM significant wave height of the Region, Sub 1 and Sub 2

Figure 6 shows the WAM significant wave height for the region, sub 1 and sub 2. The WAM model also has been calibrated with NOWPHAS observation data from Kashima Port site (35.92° N, 140.73° E). Figure 7 shows the calibration result between WAM model and field observation data at Kashima Port. After the WAM model well calibrated with observed data, then the boundary conditions for SWAN computation can be generated.
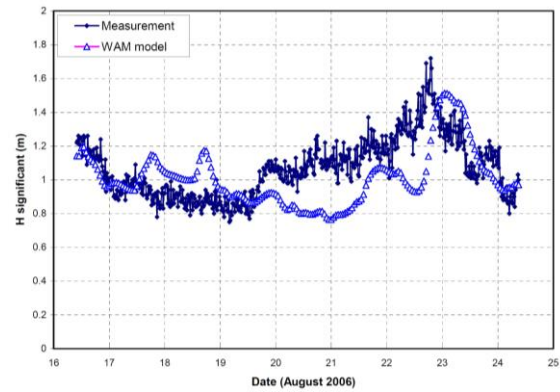
Figure 7 Comparison of significant wave heights between the WAM model and observed data at Kashima Port

In this work, SWAN has been simulated with default formulation with all the physical mechanisms such as wind generation, wave refraction, wave breaking, bottom friction, wave-wave interactions and white-capping. The performance of the SWAN computations was examined with data observations along HORS pier to calibrate the model. The comparison of significant wave height between SWAN model and significant wave height on the wave gauge locations is presented in Figure 8.
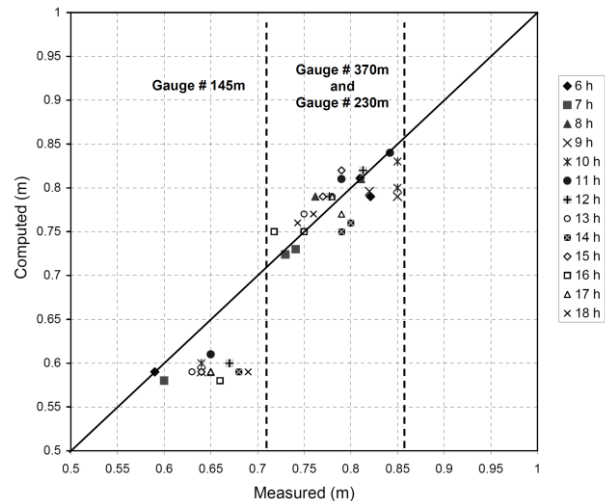
Figure 8 Significant wave heights comparison for SWAN with data observations on 18 August 2006

Figure 8 shows that SWAN simulates the significant wave height very well for two wave gauge locations (230 m and 370 m). In these two locations, the significant wave heights computed by SWAN were closer to data observations but at another location (145 m), the significant wave heights obtained by SWAN were smaller compared to in-situ wave gauge. The discrepancy results are due to the fact that at this location of 145 m, the wave breaking occurs. The phenomena of wave breaking process are difficult to model through numerical model. Another possibility is data from wave gauges are significantly affected by wave breaking in this location.
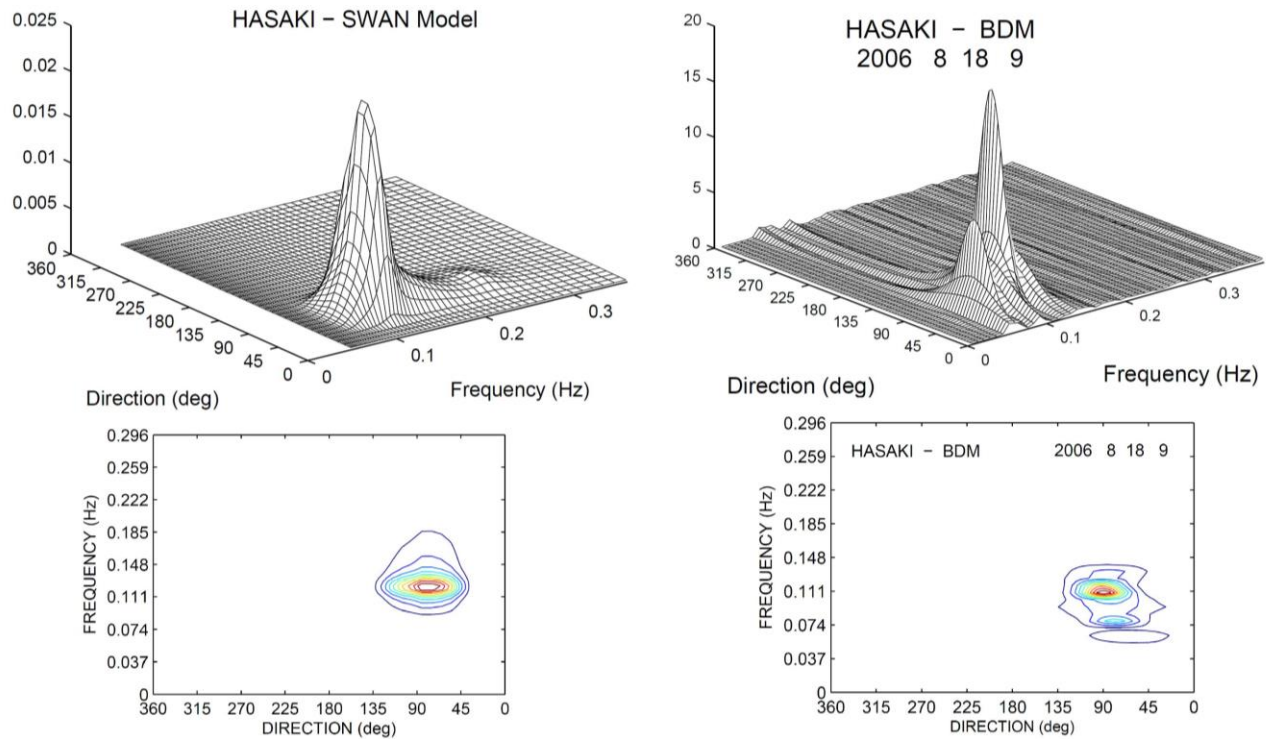
Figure 9 Directional wave spectra of swell from SWAN model (left) and from video images (right)

After the model well calibrated, directional wave spectra in shallow water can be generated as shown in Figure 9 above. Figure 9 shows the directional wave spectra generated from the SWAN model at cross shore location 230-240 m from the shoreline. The comparison of directional wave spectra results shows that there is a good agreement between directional wave spectra in shallow water estimated by SWAN and video image data. Both methods indicate that directional wave spectra are significantly narrower in frequency and direction that is typical of swell waves as indicated in both figures.

■6.0 CONCLUSION

In this paper, analysis of directional wave spectra in the shallow water area estimated by video image data has been compared with numerical wave model of SWAN. Our analysis showed that SWAN provides accurate simulation of numerical wave model and it well calibrated with data observations. Although, calibration results show that significant wave heights at area of wave breaking are underestimated.

In addition, there is a good agreement between directional wave spectra estimated by video image data and the SWAN model. Both methods estimate similar shape of directional wave spectra in the shallow water. Added, the energy distribution of the directional wave spectra in shallow water is concentrated significantly in frequency and direction.

Nomenclature

WAM   - Wave Model
SWAN   - Simulating Wave Nearshore
JMA   - Japan Meteorological Agency
HORS   - Hasaki Oceanographical Research Station
ETOPO   - Earth Model Topography
NOAA   - National Oceanic and Atmospheric and Administration
BDM   - Bayesian Directional Method
NOWPHAS - Nationwide Ocean Wave information for Port & Harbours
N - density spectrum
S_{in} - wind input
S_{nl} - non linear wave interaction
S_{wc} - wave dissipation due to white-capping
S_{bfr} - wave dissipation due to bottom friction
S_{surf} - depth-induced breaking
c - wave celerity
θ - wave direction
t - time
x/y   - x and y space

References

[1]   WAMDI Group. 1988. *J. Phys. Oceanography*. 18: 1775–1810.
[2]   Booij, N., Ris, R. C. & Holthuijsen, L. H. 1999. *Journal of Geophysical Research*. 104(C4): 7649–7666.
[3]   Aarninkhof, S. G. J. and Holman, R. A. 1999. *Backscatter*. 10(2): 8–11.

[4] Lippmann, T. C. and Holman, R. A. 1989. *Journal of Geophysical Research*. 94(C1): 995–1011.
[5] Plant, N. G. and Holman, R. A. 1997. *Marine Geology*. 140: 1–24.
[6] Holland, K. T., and Holman, R. A. 1997. *Journal of Coastal Research*. 13(1): 81–87.
[7] Stockdon, H. F., and Holman, R. A. 2000. *Journal of Geophysical Research*. 105: 22015–22033.
[8] Holman and Chickadel, C. 2004. *Proceeding of 29th ICCE*. 1072–1081.
[9] Davidson, M., Koningsveld, M. V., de Kruif, A., Rawson, J., Holman, R., Lamberti, A., Medina, R., Kroon, A. & Aarninkhof, S. 2007. *Coastal Engineering*. 54: 463–475.

[10] Zikra, M., Hashimoto, N., Yamashiro, M., Yokota, M. and Suzuki, K. 2012. *Coastal Engineering Journal*. 54(03). DOI: 10.1142/S0578563412500209.
[11] Ris, R. C., Booij, N. & Holthuijsen, L. H. 1999. *Journal of Geophysical Research*. 104(C4): 7667–7681.
[12] Zikra, M., Hashimoto, N., Yamashiro, M., Yokota, M. and Suzuki, K. 2012. Proceeding of 33rd International Conference of Coastal Engineering. ASCE. DOI: http://dx.doi.org/10.9753/icce.v33.management.43.